JOURNAL OF COMPUTATIONAL PHYSICS 23, 135–149 (1977)

On the Treatment of Advection in Flux Formulations for Variable Grid Models, with Application to Two Models of the Atmosphere*

MICHAEL C. MACCRACKEN AND ROBERT D. BORNSTEIN†

Lawrence Livermore Laboratory, University of California, Livermore, California 94550

Received April 7, 1975; revised August 13, 1975 and April 9, 1976

Numerical simulations using the flux form of the conservation equations on a nonuniform, staggered grid are shown to require careful consideration with respect to the selection of the advective velocities used to calculate the flux transport terms. Results from both a simplified form of an urban boundary layer model and from a complex global climate model demonstrate the appropriateness of the "flux-weighted" averaging technique which is presented in the paper as an alternative to linear averaging.

1. INTRODUCTION

As numerical models of the atmosphere have become more sophisticated, treatment of the advective terms has had to be improved in order to better represent real physical processes. One change has been the formulation of the advective terms in various "flux" forms by use of the incompressible form of the continuity equation. For example, the "donor cell" method [1], used in an urban boundary layer model [2], is both transportive (as the effect of a perturbation in a transported property is advected only in the direction of the velocity) and mass conservative (as the integral conservation relationships of the continuum equation are not violated [1]). Methods using centered space derivatives for the advection terms generally do not possess these properties; however, the donor cell method does somewhat retain the second-order accuracy of the centered space derivative approach while being mass conservative and transportative.

In another example of a "flux form" treatment [3], a quadratic advection scheme [4] was modified for use in a global climate model because of geometric problems encountered in a spherical coordinate system. The resulting finite difference formulation of the advective terms was identical to the quadratic scheme in the case of a constant flow on a uniform grid. However, under nonuniform conditions, the formulation possessed second-order accuracy and maintained mass consistency.

* This work was performed under the auspices of the U.S. Energy Research and Development Administration and supported in part by the Climatic Impact Assessment Program, U.S. Department of Transportation.

† Consultant with Lawrence Livermore Laboratory, permanent address: Department of Meteorology, San Jose State University, San Jose, California 95114.

ISSN 0021–9991

This paper is concerned with the application of flux methods to numerical models employing a staggered, nonuniform grid. Such models are thus able to obtain increased resolution in certain regions, and are therefore able to have velocity components represent inflow and outflow rates on various faces of particular grid volumes. In particular, a so-called "flux-weighting" technique is presented, in which the fluxes required in the finite difference analog to the advective terms are more correctly represented than those obtained from using a linear averaging scheme. Results from a simplified version of the URBMET ("urban meteorology") urban boundary layer model [2] and from the full ZAM global zonal atmospheric model [5] are presented to illustrate the effects of using the proposed technique in conjunction with two previously documented schemes.

2. Application in a Simplified Framework

The URBMET urban boundary layer model is a two-dimensional vertical plane model which has been used to study the flow over a rough, wet, warm city [6]. The model consists of two layers: (1) $0 < z \leqslant h = 25$ m, a lower analytical constant flux layer; and (2) $h < z \leqslant H = 1900$ m, an upper numerical transition layer in which the vorticity, heat, and moisture conservation equations are solved. Its grid is nonuniform and staggered, so that the two horizontal wind components, specific humidity, and the virtual potential temperature are located one-half a grid interval above and below the vorticity and streamline grid points. In addition, the grid points for the vertical component of the velocity are displaced one-half of a grid interval to the right and left of those for the vorticity.

The transition layer is assumed to be hydrostatic and Boussinesq, with the latter assumption implying incompressible flow [7]. All lateral gradients are assumed to be zero, and only adiabatic motions are considered.

The current series of simulations utilizes a simple form of URBMET, in which there is no moisture, eddy diffusion, or lateral wind component, and in which lapse rates are assumed to be adiabatic. In addition, the initial conditions specified an unrealistic, convergent flow, in which the magnitude of the horizontal wind speed varied only in the vertical. It was felt that this velocity distribution would severely test the proposed numerical schemes.

With the above assumptions, the vorticity equation in the transition layer can be written as

$$\frac{\partial \zeta}{\partial t} = -\frac{\partial}{\partial x}(u\zeta) - \frac{\partial}{\partial z}(w\zeta), \tag{1}$$

where u and w are the horizontal and vertical wind components, respectively, and where the form of vorticity ζ consistent with the hydrostatic assumption is

$$\zeta = \partial u / \partial z. \tag{2}$$

Additional details concerning the constant flux layer equations and boundary conditions are found in Appendix A.

A time splitting technique [6] is used to solve Eq. (1), in which first

$$\frac{\partial \zeta}{\partial t} = -\frac{\partial}{\partial x}(u\zeta) \tag{3}$$

is solved, and then

$$\frac{\partial \zeta}{\partial t} = -\frac{\partial}{\partial z}(w\zeta) \tag{4}$$

is solved.

A finite difference analog of Eq. (3), which is to be conservative of ζ, should relate the local time rate of change of $\zeta(i,j)$ to the difference in the fluxes into and out of the volume (Fig. 1) which surrounds grid point (i,j), e.g.,

$$\hat{\zeta}(i,j) = \zeta(i,j) - \Delta t\left[\frac{F_R - F_L}{X_R - X_L}\right], \tag{5}$$

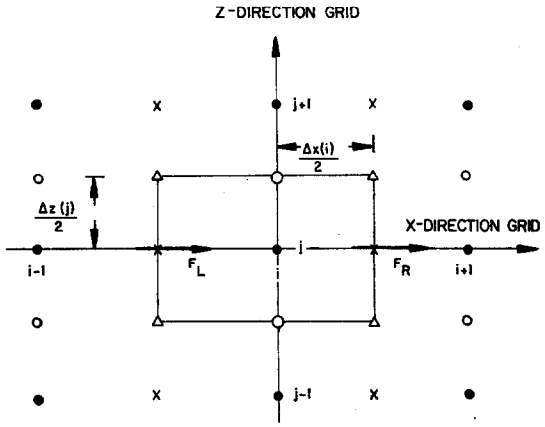

FIG. 1. Schematic representation of the horizontal fluxes in and out of the grid volume centered at the point (i,j). Also shown are the x and z direction grids, in which the advected fluid dynamic variables ζ are located at the centers of the grid volumes (shown as the dots), the "known" velocities are located halfway between the ζ-grid points (shown as the circles), and the "effective" advecting velocities u_R and u_L are located at the centers of the vertical walls perpendicular to the x- direction grid (shown as the crosses).

where the subscripts R and L refer to quantities on the right and left vertical faces of the volume whose vertical boundaries at X_R and X_L are located halfway between ζ-grid points. The fluxes F_R and F_L represent the product of a velocity and a vorticity and the cap indicates values at $(t + \Delta t)$. The magnitude of the time step Δt is computed [6] from

$$\Delta t = \left[0.75\frac{\Delta x}{u}, 0.75\frac{\Delta z}{w}\right]_{\min}, \tag{6}$$

where the horizontal and vertical grid spacings, Δx and Δz, respectively, are not constants over the entire grid, as shown in Table I.

TABLE I

Grid Locations in URBMET for u Grid Points[a]

j/i	z (m)	x (km)
1	0	−30
2	12.5	−20
3	37.5	−12.5
4	62.5	−7.5
5	87.5	−5.0
6	125	−2.5
7	175	0
8	225	2.5
9	275	5.0
10	325	7.5
11	375	10.0
12	450	15.0
13	600	22.5
14	850	32.5
15	1200	47.5
16	1650	67.5

[a] Height above the surface is in meters, indexed by j, and distance from the center of the grid is in kilometers, indexed by i.

The donor cell method is a variation on simple "upstream differencing" in that the direction of u_L and u_R determine the correct values of ζ to use in calculating the fluxes F_R and F_L to be used in Eq. (5), as follows

$$\zeta_R = \zeta(i,j), \qquad \text{for } u_R > 0, \tag{7a}$$

$$\zeta_L = \zeta(i-1,j), \qquad \text{for } u_L > 0, \tag{7b}$$

$$\zeta_R = \zeta(i+1,j), \qquad \text{for } u_R < 0, \tag{7c}$$

$$\zeta_L = \zeta(i,j), \qquad \text{for } u_L < 0. \tag{7d}$$

If a single velocity is used in forming the fluxes on the right-hand side of Eq. (5), the donor cell method reduces to the frequently used (in meteorology) simple upstream differencing technique, which has been shown to be less accurate than the donor cell method [8]. Also, if the interface values of ζ are obtained by a linear averaging technique, then the donor cell scheme becomes identical to that of centered differencing, which is nontransportive.

The velocities u_L and u_R represent "effective velocities" which must reproduce the combined effects of the flows through the upper and lower halves of the left- and right-hand faces of each volume. As shown in Fig. 2, the flow rates through the two

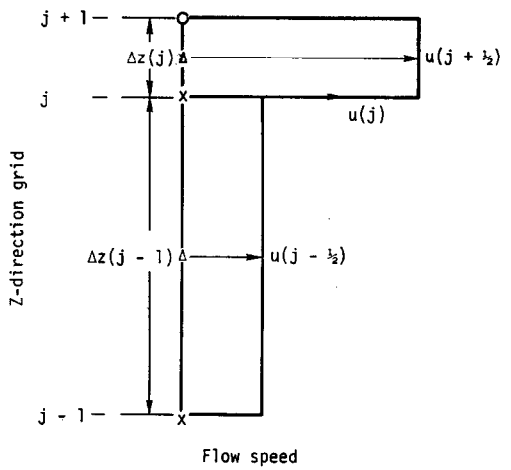

FIG. 2. Schematic representation of the vertical grid spacing and horizontal velocities at any distance along the horizontal grid. Grid points with velocities evaluated from Eqs. (8a) and (8b) (shown as triangles) are located halfway between grid points at which the "effective" advective velocities (shown as crosses) must be determined.

halves of each face are not necessarily equal, due to the use of the staggered grid. The velocities u_R and u_L are obtained by averaging the flow rates at the two adjacent ζ-grid points. As shown in Fig. 1, this leads to the following expressions.

$$u_R = u(i + \tfrac{1}{2}, j) = \tfrac{1}{2}[u(i + 1, j) + u(i, j)], \tag{8a}$$

$$u_L = u(i - \tfrac{1}{2}, j) = \tfrac{1}{2}[u(i, j) + u(i - 1, j)]. \tag{8b}$$

This simple linear averaging procedure is valid, since the vertical faces of the volume of Fig. 1, upon which the grid points for u_L and u_R are located (shown by the crosses), are exactly halfway between successive ζ-grid points (shown by the dots).

The main concern of this paper is the formulation of the appropriate weighting scheme to be used to calculate the correct velocities appearing in the extreme right-hand terms of Eqs. (8a) and (8b) (which are located on the j grid line) from the "known" velocities (located on the $(j \pm \frac{1}{2})$ grid lines) and shown by the circles in Fig. 1. An obvious approach is through linear interpolation, e.g.,

$$u(i, j) = \frac{\Delta z(j - 1)\, u(i, j + \frac{1}{2}) + \Delta z(j)\, u(i, j - \frac{1}{2})}{\Delta z(j) + \Delta z(j - 1)}, \tag{9}$$

where

$$\Delta z(j) \equiv z(j + 1) - z(j).$$

Use of Eq. (9) in conjunction with a similar expression for $u(i + 1, j)$ in Eq. (8a) yields the following form for u_R

$$u_R = \{\Delta z(j - 1)[u(i + 1, j + \tfrac{1}{2}) + u(i, j + \tfrac{1}{2})] + \Delta z(j)[u(i + 1, j - \tfrac{1}{2}) + u(i, j - \tfrac{1}{2})]\}/[\Delta z(j) + \Delta z(j - 1)]. \tag{10}$$

Application of the simple linear averaging technique expressed in Eqs. (8a) and (8b) to the velocities in Eq. (10) yields

$$u_R = \frac{\Delta z(j-1)\, u(i+\frac{1}{2}, j+\frac{1}{2}) + \Delta z(j)\, u(i+\frac{1}{2}, j-\frac{1}{2})}{\Delta z(j) + \Delta z(j-1)}, \tag{11}$$

where $u(i+\frac{1}{2}, j \pm \frac{1}{2})$ are the velocities midway between $u(i, j \pm \frac{1}{2})$ and $u(i+1, j \pm \frac{1}{2})$.

For a positive value of u_R, in association with the donor cell scheme, F_R is therefore given by

$$F_R = u_R \zeta(i, j). \tag{12}$$

For the limiting case in which $\Delta z(j)$ approaches zero, Eq. (9) indicates that $u(i, j)$ approaches $u(i, j+\frac{1}{2})$. As shown in Fig. 2, this might be a reasonable estimate for $u(i, j)$, because of its close proximity to $u(i, j+\frac{1}{2})$. However, the limiting value of Eq. (12), when u_R is given by Eq. (11), is given by

$$F_R = u(i+\tfrac{1}{2}, j+\tfrac{1}{2})\zeta(i, j). \tag{13}$$

This is not a reasonable estimate of the flux under the same conditions, because most of the fluid, based on the division of the region into cells, as shown in Fig. 2, is really moving with the speed of $u(i+\frac{1}{2}, j-\frac{1}{2})$.

The approach here proposed for obtaining the correct "effective velocity" takes note of the discrete nature of the fluid structure which is created by finite differencing. Since the fluid in region $\Delta z(j)$ is moving with a speed of $u(i+\frac{1}{2}, j+\frac{1}{2})$, while that of $\Delta z(j-1)$ is moving at $u(i+\frac{1}{2}, j-\frac{1}{2})$, a conservative, or "flux-weighting," averaging procedure leads directly to the following expression for $u(i, j)$ (as seen from Figs. 1 and 2).

$$u(i, j) = \frac{\Delta z(j)\, u(i, j+\frac{1}{2}) + \Delta z(j-1)\, u(i, j-\frac{1}{2})}{\Delta z(j) + \Delta z(j-1)}. \tag{14}$$

Application of the procedure expressed in Eq. (14) to both of the velocities on the right-hand side of Eq. (8) leads directly to

$$u_R = \frac{\Delta z(j)\, u(i+\frac{1}{2}, j+\frac{1}{2}) + \Delta z(j-1)\, u(i+\frac{1}{2}, j-\frac{1}{2})}{\Delta z(j) + \Delta z(j-1)}. \tag{15}$$

When $\Delta z(j)$ is again hypothesized to approach zero, and when Eq. (15) is used for u_R in Eq. (12), the flux now approaches

$$F_R = u(i+\tfrac{1}{2}, j-\tfrac{1}{2})\zeta(i, j). \tag{16}$$

As shown in Fig. 2, the above expression is a better estimate of F_R than that given by Eq. (13), as most of the fluid is now moved with the speed $u(i+\frac{1}{2}, j-\frac{1}{2})$. However, the new estimate of $u(i, j)$ obtained from the limiting value of Eq. (14) is $u(i, j-\frac{1}{2})$, which is not as reasonable as that given in the previous case, because of the large value of $\Delta z(j-1)/2$ shown in Fig. 2.

Given the discrete nature of finite difference solutions, perhaps the best estimate of $u(i,j)$, when it is *not* needed for a flux computation, is simply (as seen in Fig. 2) to set it equal to the average of the rates at which the fluid is moving immediately above and below that level, i.e.,

$$u(i,j) = \tfrac{1}{2}[u(i,j+\tfrac{1}{2}) + u(i,j-\tfrac{1}{2})]. \tag{17}$$

Note that both Eqs. (9) and (14) yield the above expression in the case of a uniform grid spacing, and that both Eqs. (12) and (15) also yield identical expressions for u_R and hence F_R under that special condition. A similar procedure must be followed for F_L in Eq. (5) and for the fluxes in the vertical advection terms of Eq. (4). Details of the solution for the velocity components and for the constant flux layer variables are found in Appendix A.

For the simple case described here, the initial wind field consisted of the u-components of an equilibrium Ekman-type wind spiral for the case of a geostrophic wind U of 3 m sec^{-1} and a surface roughness length of 50 cm. The vertical variation of the eddy viscosity coefficient $K(z)$ was evaluated using a third-order polynomial [9].

The absolute magnitude of $u(z)$ at a grid level j was initially constant, but negative values were specified at all grid points at $i > 7$. Thus the flow was initially specified to converge at a line midway between grid columns 7 and 8, i.e., at $x = -1.25$ km. Hence the w-field was initially zero at all grid locations, except those at the line of convergence where the values were positive. A maximum value of 4.45 m sec^{-1} was found at the upper most grid level.

Results obtained using the simplified form of URBMET in conjunction with the "flux weighted" form of $u(i,j)$ given by Eq. (14) and with the "linear weighted" form given by Eq. (9) are shown in Figs. 3 and 4, respectively. The vertical velocity field was selected for presentation because it clearly demonstrates the effect of using the correct weighting scheme when the value of a parameter at a grid point must be computed so as to represent the mean value over a grid interval. With the "linear weighted" form, the values change sign at adjacent horizontal grid locations, while with the "flux weighted" form, a more coherent pattern results.

3. Application in a Full Model of the Atmosphere

A more accurate second-order alterantive to the donor cell formulation of an advective flux term, and the one used in the ZAM model, can be derived by integrating in time and assuming that any fluid dynamic variable ζ varies linearly from i to $(i+1)$. The flux at $(i+\frac{1}{2})$ is then the integral of ζ from $(x_R - u_R \Delta t)$ to x_R. This gives

$$F_R = \frac{1}{\Delta t} \int_{x_R - u_R \Delta t}^{x_R} \zeta(x')\, dx', \tag{18}$$

where

$$\zeta(x') = (\zeta_{i+1} - \zeta_i) \frac{x'}{\Delta x(i)} + \zeta_i, \tag{19}$$

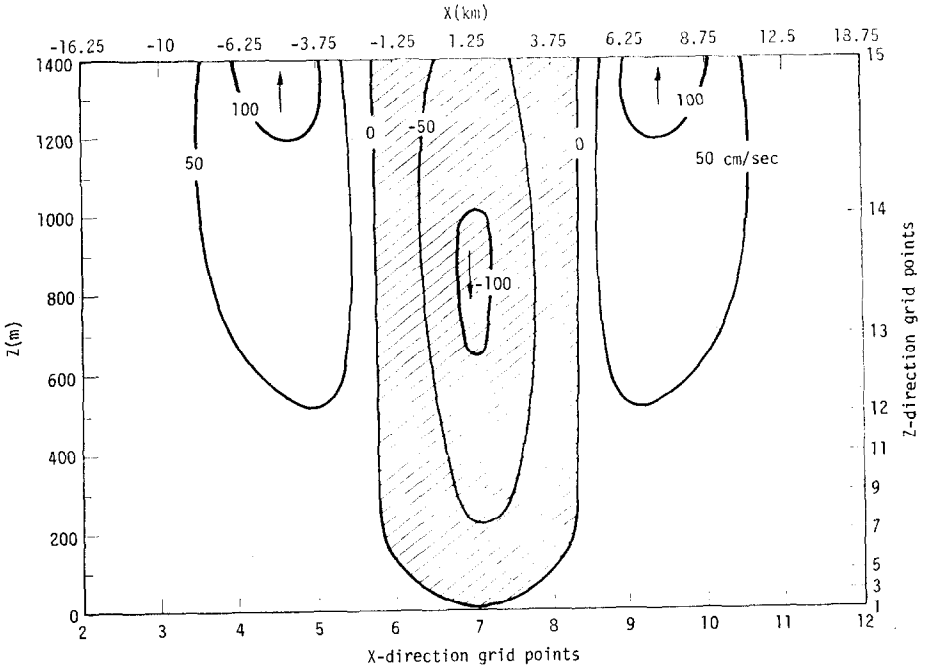

FIG. 3. The vertical velocity field computed from the URBMET model after 6 hours of simulated time using "flux-weighted" averaging to calculate the "effective" advective velocities.

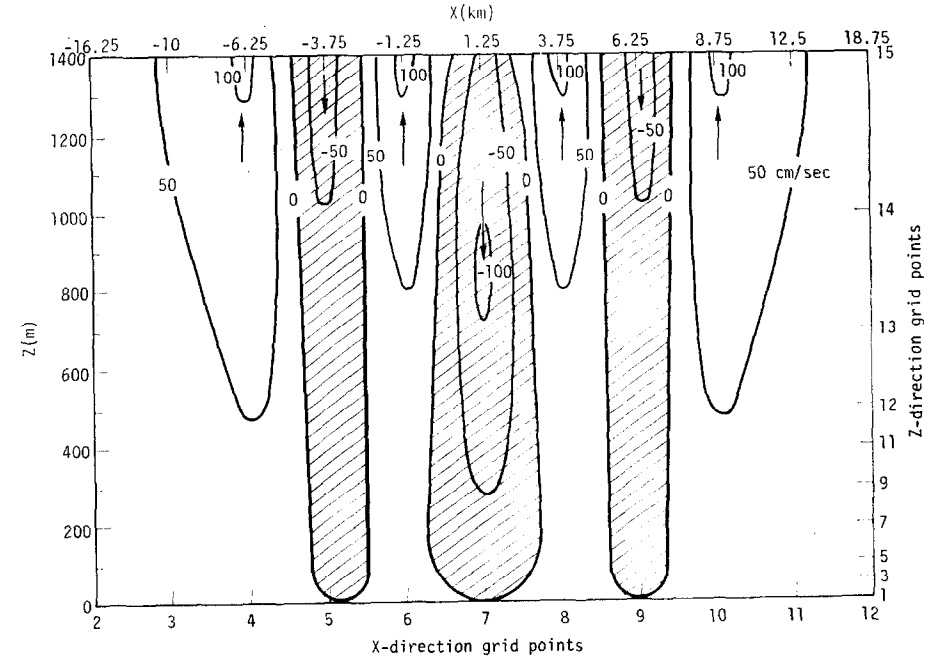

FIG. 4. The vertical velocity field computed from the URBMET model after 6 hr of simulated time using linear-averaging to calculate the "effective" advective velocities.

and

$$\Delta x(i) \equiv x(i+1) - x(i). \tag{20}$$

Performing the integration yields

$$F_R = \frac{1}{\Delta t}\left[(\zeta_{i+1} + \zeta_i)\frac{u_R \Delta t}{2} - (\zeta_{i+1} - \zeta_i)\frac{(u_R \Delta t)^2}{2\Delta x(i)}\right]. \tag{21}$$

Note that, if we now calculate the change in concentrations in grid cell i due to fluxes on the right and left faces, as indicated in Eq. (5), with the following assumptions

$$u = u_R = u_L \tag{22}$$

and

$$\Delta x = \Delta x(i-1) = \Delta x(i+1) = \Delta x(i), \tag{23}$$

then Eq. (5) becomes

$$\left(\frac{\Delta \zeta}{\Delta t}\right)_{i,j} = \frac{1}{\Delta t}\left[(\zeta_{i-1} - \zeta_{i+1})\frac{u \Delta t}{2\Delta x} + 2(\zeta_{i+1} - 2\zeta_i + \zeta_{i-1})\left(\frac{u \Delta t}{2\Delta x}\right)^2\right]. \tag{24}$$

This is the quadratic advection scheme for a regular grid [4], derivable by use of a Taylor expansion of ζ in x about $x(i)$, followed by an evaluation of ζ at $[x(i) - u \Delta t]$, i.e., at the point which will be advected to $x(i)$ during time step Δt.

The assumptions required to obtain the quadratic form, however, may not always be valid (e.g., for a nonuniform velocity, nonrectangular grid, etc.), and it is more conservative of the variable ζ to calculate the fluxes at each edge of the cell, and then take the divergence. It is quickly seen why use of a staggered grid is appropriate, since the velocity is needed at the $(i \pm \frac{1}{2})$ grid points. In two-dimensional models, the velocities are also usually offset in the second dimension for similar reasons.

The ZAM zonal atmospheric model is a two-dimensional (latitude and vertical) global model developed to simulate the latitudinal variation of world climate. The model treats a moist atmosphere including precipitation and clouds, and has a detailed radiation calculation. Of relevance to this paper is that it computes the evolution of temperature, water vapor, surface pressure, and zonal and meridional winds using the appropriate conservation equations in their primitive form. This extensive intercoupling precludes simplifying this model to treat just the single equation discussed in the previous section. The grid in the ZAM model is staggered such that temperature is defined at so-called even latitudes and even pressure levels, and the wind components are defined at odd latitudes and odd pressure levels. Although the latitude intervals are evenly spaced at 10°, the vertical levels are not evenly spaced in pressure coordinates (but are approximately evenly spaced in altitude).

In the three-dimensional atmospheric model of [4], the quadratic advection scheme given by Eq. (24) was used, and the resulting lack of conservation was small and could be tolerated because the computer runs were for reasonably short time periods, and because surface temperatures were held fixed (thus providing a buffer for energy balance errors). In assuring the necessary energy balances needed for the long-term

climate studies carried out with the ZAM model under conditions of varying surface temperature, it has been found necessary to use the flux form expressed in Eq. (21). In the implementation of this equation, the need for the proper "effective velocity" for advection of the temperature (that is, determining what velocity to use at the odd latitude, even pressure level) can best be illustrated by an example.

Using the "flux-weighted" form of $u(i,j)$ given by Eq. (14), the model produces reasonable and smooth patterns of the various field variables over very long runs (years of simulated time), as shown in Figs. 5 and 6. (The apparent absence of the

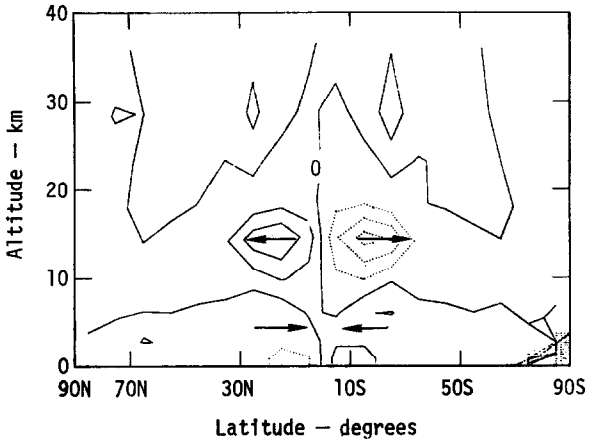

FIG. 5. The near steady-state meridional velocity field computed from the ZAM model, after 1 year of simulated time, using "flux-weighted" averaging to calculate the "effective" advective velocities. Solid contours are northerly flow, dotted contours are southerly. The contour interval is 1 km hr^{-1}.

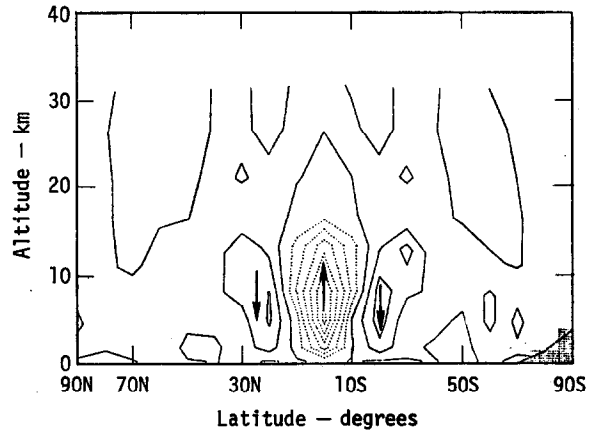

FIG. 6. The near steady-state vertical velocity field computed from the ZAM model, after 1 year of simulated time, using "flux-weighted" averaging to calculate the "effective" advective velocities. Solid contours are downward flow, dotted contours are upward flow. The contour interval is 1 decapascals hr^{-1}.

mid-latitude Ferrel cell is a result of the use in this study of an annual average model, thus not providing for the averaging of circulation over an annual solar cycle which gives the appearance of the Ferrel cell.)

If the method of calculating the velocity is switched to the linear average given by Eq. (9), however, within 24 time steps (a simulated time of 12 hours), the wind and temperature fields break down into 10° (i.e., single grid spacing) wide convective cells, as shown in Figs. 7 and 8. A complete breakdown occurs after about 16 more time steps. It is interesting that the advection of temperature is the term which excites the

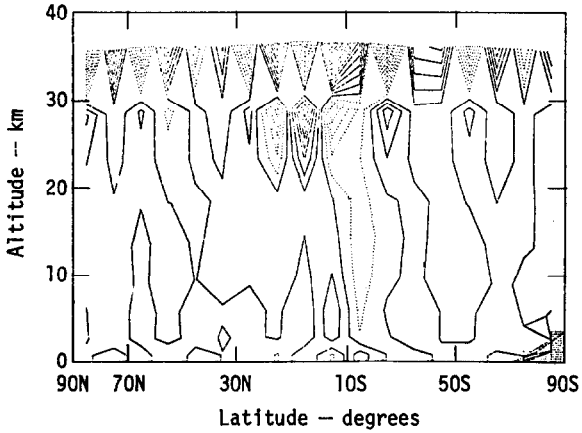

FIG. 7. The meridional velocity field computed from the ZAM model, after 12 hours of simulated time (starting from the near steady-state conditions of Fig. 5), using linear-averaging to calculate the "effective" advective velocities. Solid contours are northerly flow, dotted contours are southerly. The contour interval is 2 km hr^{-1}.

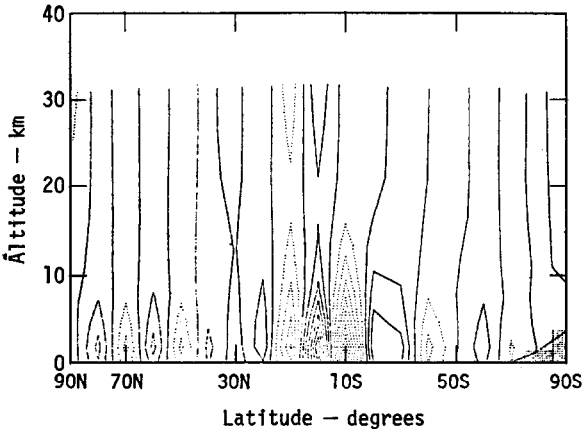

FIG. 8. The vertical velocity field computed from the ZAM model, after 12 hours of simulated time (starting from the near steady-state conditions of Fig. 6), using linear-averaging to calculate the "effective" advective velocities. Solid contours are downward flow, dotted contours are upward. The contour interval is 4 decapascals hr^{-1}.

convective cells through the coupling of wind and temperature via the hydrostatic equation.

As shown in Fig. 9, this breakdown is a quite separate phenomenon from problems such as nonlinear instability. The graph presents the time history of surface temperature at the equator for the following four cases: (1) "flux-weighted" averaging with a time step of 0.5 hr; (2) linear averaging with a time step of 0.5 hr; (3) "flux-weighted" averaging with a time step of 1.0 hr; and (4) linear averaging with a time step of 0.25 hr.

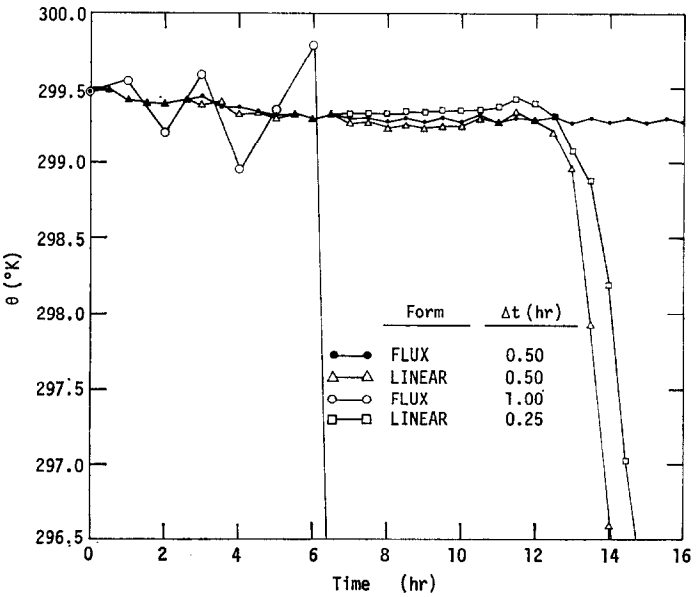

FIG. 9. Time history of surface temperature at the equator for the four cases discussed in text, starting from the near steady-state conditions of Figs. 5 and 6.

The results of Case 1 show small adjustments occurring at each time step as the solution evolves to a steady state. Similar results are obtained in Case 2 during the first 12 hr of the simulation, but beyond that time, the solution becomes unstable exponentially once the instability is initiated.

The difference between the instability of Case 2 and the so-called "time-step" computational instability (Case 3) is the difference between exponential growth and oscillatory growth. When the time step for the linear averaging case was reduced by a factor of two (Case 4), the results diverged from the solution of Case 1 at about the same time step as in Case 2.

Had the instability of the solution in Case 2 been due to "time-step" computational instability, then the instability of Case 4 would have occurred much later than when it occurred in Case 2. Had the instability of Case 2 been related to the number of time steps, then the instability of Case 4 would have occurred after about 6 hr of simulated time. Other possible causes for the instability of Cases 2 and 4, such as inconsistent calculation of the vertical velocity, have been studied and ruled out.

4. Summary

The increasingly widespread use of the flux form of the conservation equations in numerical simulations (because of its numerical advantages and conservative properties) is shown to require careful consideration when utilized in conjunction with a nonuniform, staggered grid. In particular, careful attention must be paid so that the value of a parameter at a grid point will be calculated so as to represent the mean value of that parameter over its grid interval *when* that value is to be used in a flux computation.

A linear averaging approach to specifying "effective" advective velocities results in a representative velocity, but an unrepresentative flux, and leads to grid-sized convective motions in both a global climate model and an urban boundary layer model. Use of a proposed "flux-weighted" effective velocity, which takes cognizance of the discrete nature of fluids resulting from finite differencing, leads to smoother and more realistic motion fields in the two models for which comparisons were made.

APPENDIX A: Details of Simplified URBMET Model

Since the flow is incompressible, u and w are related to a stream function ψ by

$$u = \partial\psi/\partial z, \tag{A1}$$

$$w = -\partial\psi/\partial x, \tag{A2}$$

and thus from Eqs. (2) and (A1)

$$\zeta = \partial^2\psi/\partial z^2. \tag{A3}$$

In the analytical surface boundary layer, the following form of the logarithmic wind profile is assumed.

$$u = \frac{u_*}{k_0} \ln\left(\frac{z + z_0}{z_0}\right), \tag{A4}$$

where u_* is the friction velocity, z_0 is the specified surface roughness parameter, taken as 50 cm, and k_0 is the von Karman constant, taken as 0.4.

The following boundary conditions are assumed.

At $z = 0$,

$$u = \partial\psi/\partial z = 0, \tag{A5}$$

$$w = -\partial\psi/\partial x = 0, \tag{A6}$$

which imply a constant value of ψ, taken as zero for convenience;

At $z = h$,

$$\text{continuity of } u \text{ and } \partial u/\partial z; \tag{A7}$$

At $z = H$,

$$u = \partial\psi/\partial z = \pm U, \tag{A8}$$

$$\partial u/\partial z = \zeta = \partial^2\psi/\partial z^2 = 0, \tag{A9}$$

where U, taken as $+3$ m sec^{-1} in the left half of the model, changes sign in the right half of the model.

The continuity condition of Eq. (A7) is given as

$$\frac{u(3h/2) - u(h/2)}{\Delta z} \approx \left(\frac{\partial u}{\partial z}\right)_h, \tag{A10}$$

where near the surface Δz has the same magnitude as h. The value of $u(3h/2)$ is known from the finite difference solution, while $u(h/2)$ and $(\partial u/\partial z)_h$ are obtained from Eq. (A4) and its vertical derivative. When these substitutions are made in Eq. (A10), and the resulting expression solved for u_*, the following is obtained.

$$u_* = \frac{k_0(h + z_0)\, u(3h/2)}{h + (h + z_0)\ln[(0.5h + z_0)/z_0]}. \tag{A11}$$

The system of equations is solved at a given time step on the grid given in Table I as follows: u_* from Eq. (A11); $u(h/2)$ and $(\partial u/\partial z)_h$ from Eq. (A4) and its vertical derivative; ζ from Eqs. (3) and (4); ψ from (A3), using a form of the Gaussian elimination [10] method which has been modified to take into account the variable nature of the grid; and, finally, u and w from the finite difference analogs to Eqs. (A1) and (A2)

$$\hat{u}(i, j + \tfrac{1}{2}) = \frac{\hat{\psi}(i, j + 1) - \hat{\psi}(i, j)}{\Delta z(j)} \tag{A12}$$

and

$$\hat{w}(i + \tfrac{1}{2}, j) = \frac{\hat{\psi}(i, j) - \hat{\psi}(i + 1, j)}{\tfrac{1}{2}[\Delta x(i) + \Delta x(i + 1)]}. \tag{A13}$$

Note that the velocity in Eq. (A12) is that appearing on the right-hand side of Eq. (9).

References

1. P. J. Roach, "Computational Fluid Dynamics," Hermosa, Albuquerque, New Mexico, 1972.
2. R. D. Bornstein, The two-dimensional URBMET urban boundary layer model, *J. Appl. Meteorol.* **14** (1975), 1459–1477.
3. M. C. MacCracken, Ice age theory analysis by computer model simulation, Ph.D. thesis, University of California, Davis/Livermore, 1968.
4. C. E. Leith, Numerical simulation of the earth's atmosphere, *Methods Comp. Phys.* **4** (1965), 1–28.
5. M. C. MacCracken and F. M. Luther, Climate studies using a zonal atmospheric model, Proceedings of the IAMAP/IAPSO First Special Assembly, Melbourne, Australia, January 1974.

6. R. D. BORNSTEIN AND A. D. ROBOCK, Effects of variable and unequal time steps in the simulation of the urban boundary layer using the two-dimensional "URBMET" model, *Mon. Weather Rev.* **104** (1976), 260–267.
7. F. A. SPIEGEL AND G. VERONIS, On the Boussinesq approximation for a compressible fluid, *Astrophys. J.* **131** (1960), 442–447.
8. K. E. TORRENCE, Comparison of finite-difference computations of natural convection, *J. Res. of the Natl. Bur. Stand.* **72B**, 4 (1968), 281–301.
9. J. O'BRIEN, On the vertical structure of the eddy exchange coefficient in the planetary boundary layer, *J. Atmos. Sci.* **27** (1970), 1213–1215.
10. R. D. RICHTMYER, "Difference Methods for Initial-Value Problems," Interscience, New York, 1957.